The Astrophysical Journal, 600:390–403, 2004 January 1


# THEORETICAL MODELING OF THE THERMAL STATE OF ACCRETING WHITE DWARFS UNDERGOING CLASSICAL NOVA CYCLES

Dean M. Townsley
Department of Physics, Broida Hall, University of California, Santa Barbara, CA 93106; townsley@physics.ucsb.edu

and

Lars Bildsten
Kavli Institute for Theoretical Physics and Department of Physics, Kohn Hall, University of California, Santa Barbara, CA 93106; bildsten@kitp.ucsb.edu
*Received 2003 June 3; accepted 2003 September 3*

## ABSTRACT

White dwarfs (WDs) experience a thermal renaissance when they receive mass from a stellar companion in a binary. For accretion rates of less than $10^{-8}\ M_\odot\ \mathrm{yr}^{-1}$, the freshly accumulated hydrogen/helium envelope ignites in a thermally unstable manner that results in a classical nova (CN) outburst and ejection of material. We have undertaken a theoretical study of the impact of the accumulating envelope on the thermal state of the underlying WD. This has allowed us to find the equilibrium WD core temperatures ($T_c$), the CN ignition masses ($M_{\rm ign}$), and the thermal luminosities for WDs accreting at rates of $10^{-11}$ to $10^{-8}\ M_\odot\ \mathrm{yr}^{-1}$. These accretion rates are most appropriate for WDs in cataclysmic variables (CVs) of $P_{\rm orb} \lesssim 7$ hr, many of which accrete sporadically as dwarf novae. We have included $^3$He in the accreted material at levels appropriate for CVs and find that it significantly modifies the CN ignition mass. We compare our results with several others from the CN literature and find that the inclusion of $^3$He leads to lower values of $M_{\rm ign}$ for $\langle \dot{M} \rangle \gtrsim 10^{-10}\ M_\odot\ \mathrm{yr}^{-1}$ and that for $\langle \dot{M} \rangle$ values below this the particular author's assumption concerning $T_c$, which we calculate consistently, is a determining factor. Initial comparisons of our CN ignition masses with measured ejected masses find reasonable agreement and point to ejection of material comparable to that accreted.

*Subject headings:* binaries: close — novae, cataclysmic variables — nuclear reactions, nucleosynthesis, abundances — stars: dwarf novae — white dwarfs

## 1. INTRODUCTION

Classical novae (CNs) are the result of unstable thermonuclear ignition of freshly accreted hydrogen and helium on a white dwarf (WD) in a mass-transferring binary. The orbital periods of these binaries presently range from 1.4 to more than 16 hr, with a large number in the 2–4 hr range (Diaz & Bruch 1997; Warner 2002). These cataclysmic variables (CVs; Warner 1995) have low-mass stellar companions and spend most of their lives accreting at time-averaged rates $\langle \dot{M} \rangle \approx 10^{-9}$ to $10^{-11}\ M_\odot\ \mathrm{yr}^{-1}$ (e.g., Howell, Nelson, & Rappaport 2001). The frequency of CNs as a function of orbital period depends on the accumulated mass immediately prior to the explosion, $M_{\rm ign}$. However, the value of $M_{\rm ign}$ strongly depends on the WD's core temperature $T_c$, which is a priori unknown and must be either calculated or measured. Knowledge of the ignition mass is also needed for comparisons with measured ejected masses in CNs that would decide whether or not the underlying carbon/oxygen WD is being excavated during the CN event.

CVs are formed when the WD made during a common-envelope event finally comes into contact with its companion as a result of gravitational radiation losses over a few gigayears (e.g., Howell et al. 2001). The WD will have cooled during this time; a $0.20\ M_\odot$ He WD would have $T_c = 3.3 \times 10^6$ K at 4 Gyr (Althaus & Benvenuto 1997), whereas a $0.6\ M_\odot$ C/O WD would have $T_c = 2.5 \times 10^6$ K in 4 Gyr (Salaris et al. 2000). These WDs would have effective temperatures $T_{\rm eff} \approx 4500$–$5000$ K. A subset of the CVs, called dwarf novae (DNs), contain a WD accreting at low time-averaged rates $\langle \dot{M} \rangle < 10^{-9}\ M_\odot\ \mathrm{yr}^{-1}$, where the accretion disk is subject to a thermal instability that causes it to rapidly transfer matter onto the WD (at $\dot{M} \gg \langle \dot{M} \rangle$) for roughly a week once every month to year. The value of $\dot{M}$ onto the WD is low enough between outbursts that the UV emission is dominated by the internal luminosity of the WD, allowing for a measurement of $T_{\rm eff} > 10,000$ K (Sion 1999). This is the best evidence that the WD is hotter than a cooling WD of similar age because of the thermal impact of accretion. Sion (1995) has argued that most of this heating is from gravitational energy released (i.e., converted to thermal energy) in the WD interior via material compression. This energy is then transported outward to the stellar surface, and we find that it can similarly heat the core. We will discuss this in great detail, as well as explain the important role of nuclear "simmering." A thorough comparison of our theoretical work with $T_{\rm eff}$ observations and a summary of the implications for CV evolution are in a companion paper (Townsley & Bildsten 2003).

The gravitational energy released ($GM/R$) when a particle falls from a large distance to the stellar surface, sometimes termed the "accretion energy," is deposited at or near the photosphere and is rapidly radiated away. This energy does not get taken into the star, since the time it takes the fluid to move inward is always much longer than the time it takes for heat to escape. This basically eliminates the outer boundary condition and instead points to the importance of energy released deep in the WD because of both gravitational energy released via compression within the star and hydrostatic nuclear burning.

This energy takes a long time to exit, is still visible when accretion has halted, sets $T_{\rm eff}$, and reheats the WD.

We begin in § 2 by explaining the physics of heating within the accreted envelope and how it differs from heating in the deep core (discussed in Appendix A). Since these WDs are accreting at rates low enough that the accumulated hydrogen burns unstably, we also need to carefully track the accumulated mass of material and account for the additional energy source of slow nuclear simmering near the base of the accreted layer. This is significant since the layer accumulates and eventually triggers the CN. The calculation of $M_{\rm ign}$ for a fixed $T_c$ is explained in § 3 (closely comparing with the original Fujimoto 1982 work), where we also exhibit the importance of the $^3$He content in the accreting material.

Our method of finding the equilibrium WD core temperature (Townsley & Bildsten 2002) is explained in § 4 and improves on that of Iben, Fujimoto, & MacDonald (1992a) by allowing the accreted envelope mass to change through the CN cycle. We show that early in the cycle, when the mass of the newly accreted layer is small, compressional heating is small and the WD cools. Later in the cycle, the accreted layer becomes thick enough that compressional heating along with nuclear simmering heats the core. Thus, the core cools at low accumulated masses and is heated prior to unstable ignition. Using CN ignition conditions to determine the maximum mass of the overlying freshly accreted shell, we then find the steady-state, (i.e., cooling equals heating throughout the CN cycle) core temperature $T_{c,\rm eq}$ as a function of $\langle \dot{M} \rangle$ and $M$. We close § 4 by showing that for $\langle \dot{M} \rangle \lesssim 10^{-9}\ M_\odot\ {\rm yr}^{-1}$ the WD reaches this equilibrium after accreting an amount of mass less than its own and that in CVs with $P_{\rm orb} \lesssim 2$ hr the accretion rate changes slowly enough that the WD should always be near the equilibrium given by $\langle \dot{M} \rangle$ and $M$.

Having found the core temperatures, we then predict the amount of mass that needs to accumulate on the WD in order to unstably ignite the accumulated hydrogen as a function of $\langle \dot{M} \rangle$ and $M$. Our work is compared with previous calculations in § 5, where we find very large differences with others due to their lack of knowledge of $T_c$. We also compare our predictions of $M_{\rm ign}$ with those few measures of the ejected masses in CNs of known orbital period. Within the confines of this limited comparison, we find that the ejected masses are comparable with the amount accumulated. The equilibrium also yields powerful relations between the WD surface temperature and its accretion rate and mass. These allow tests of binary evolution models as well as measures of the masses of these WDs; a comparison to the accumulated observations of effective temperatures in the DN systems is being published separately (Townsley & Bildsten 2003). We close with a summary and discussion of future work, especially the seismology of these accreting WDs.

## 2. ATMOSPHERIC MODEL INCLUDING ACCRETION

Starting with Mestel (1952), single-WD atmospheres have been characterized by a relation between the surface luminosity $L$ and the core temperature $T_c$ (e.g., Wood 1995; Hansen 1999; Chabrier et al. 2000; Salaris et al. 2000). This is one of two components (the other being the thermal content of the core) needed for evolutionary calculations of a cooling WD. In this case the atmosphere extends to the location where electron conduction forces the core to be isothermal. This occurs at $M_{\rm env} = 5 \times 10^{-5}\ M_\odot$ for $T_c = 4 \times 10^6$ K and $M = 0.6\ M_\odot$ when $L = 3 \times 10^{-4}\ L_\odot$ (see Fig. 1 in Fontaine, Brassard, & Bergeron 2001).

In an accreting WD, energy is released in the atmosphere by the slow downward motion of matter in the gravitational field and by a slow rate of hydrogen fusion. This internal energy release modifies the $L$-$T_c$ relation, giving an accreting WD a higher value of $L$ than a nonaccretor of the same $T_c$. The $L$-$T_c$ relation of nonaccreting WDs depends on the surface gravity $g$, which is set by the mass $M$, and on the composition of the envelope (which fixes the opacity), typically split into layers of pure H and He. The WD mass enters in much the same way in the accreting case, but the composition also determines the local energy release in the envelope. We parameterize composition by the mass of the freshly accreted layer $M_{\rm acc}$, which has the composition of the donor star. We use a solar composition with mass fractions $X_{\rm H} = 0.709$, $X_{^4{\rm He}} = 0.271$, $X_{\rm C} = 0.009$, and $X_{\rm O} = 0.011$. Since $^3$He will prove important as an ignition trigger (see discussion in § 3) at low values of $\langle \dot{M} \rangle$, we will show models with $X_{^3{\rm He}} = 0.001$ and 0.005, the lower and upper limits on expected values for the accreted material (e.g., D'Antona & Mazzitelli 1982; Iben & Tutukov 1984). Interior to this layer we assume a C/O core. As material is accreted at a time-averaged rate $\langle \dot{M} \rangle$, $M_{\rm acc}$ varies from zero (immediately after a CN event) to some maximum $M_{\rm ign}$ just before ignition of the next CN. Thus three parameters, $M$, $M_{\rm acc}$, and $\langle \dot{M} \rangle$, lead to an $L$-$T_c$ relation.

Because of the deposition of energy in the envelope, the surface luminosity is not equal to the thermal energy lost by the degenerate core. However, the atmospheric model provides not only $L$ at the surface but also the luminosity $L_{\rm core}$, which enters the bottom of the atmosphere from the core. This luminosity couples the envelope model to the thermal content of the core, determining the temporal evolution of $T_c$. As we will show, when $T_c$ is low, the envelope heats the degenerate core and $L_{\rm core} < 0$.

### 2.1. *Thin-Shell Approximation*

As a spherical, gravitationally self-bound object accretes matter, it undergoes structural changes that we divide into two types: (1) global structural changes that affect the core radius and (2) internal movements of material. See Nomoto (1982) and Appendix A for a discussion of the distinction between these terms. In the outer parts of the WD, the two effects are largely decoupled; material moves through the envelope and down into a deeper reservoir, and the WD radius and the gravitational field in which the envelope exists are set by the total WD mass. This is particularly useful for the case of low values of $\langle \dot{M} \rangle$, where the global changes happen extremely slowly and can therefore be safely neglected. Our treatment of the core is presented in Appendix A, where we show that the energy release in the envelope dominates that in the core by a factor of $\simeq$5.

Within a thin shell near the surface, accreted material enters at the top and displaces preexisting material that moves "out" of the shell, deeper into the star. With the assumption that the radius and total stellar mass, and thus $g$, are fixed on the timescale being considered, the local heat equation becomes

$$T \frac{Ds}{Dt} = T \frac{\partial s}{\partial t} + T v_r \frac{\partial s}{\partial r} = -\frac{dL}{dM_r} + \epsilon_N\ , \qquad (1)$$

where $\epsilon_N$ is the nuclear burning rate, $s$ is the entropy per gram, and $v_r = -\langle \dot{M} \rangle / 4\pi r^2 \rho$ is the downward speed of material

motion in response to accretion. If a fluid element loses entropy as it is compressed, then that liberated energy is carried away by heat transport. The thermal structure of the envelope determines the two spatial derivatives and the nuclear energy input in equation (1). Thus $\partial s/\partial t$, the time evolution of the entropy field, depends on the current thermal structure and $\langle \dot{M} \rangle$. A thermal structure for which $\partial s/\partial t = 0$ is a static state for the envelope. If a higher value of $\langle \dot{M} \rangle$ were applied without changing the thermal structure, a local buildup of heat would occur, $\partial s/\partial t > 0$, because of the increase of $|v_r|$ without a change in $dL/dM_r$. A lower value of $\langle \dot{M} \rangle$ leads to a corresponding cooling of the envelope. When the entropy advection term dominates over the nuclear burning term, this static state is stable because $L$ has a stronger temperature dependence than $s$ in both degenerate and nondegenerate regimes. However, when $\epsilon_N$ dominates over the advection, a thermal instability is likely, leading to a CN explosion.

The radial derivative is evaluated from the envelope structure. We work in pressure coordinates and define $\dot{m} = \langle \dot{M} \rangle / 4\pi r^2$, so

$$T v_r \frac{ds}{dr} = g\dot{m}T \frac{ds}{dP} = \frac{g\dot{m}c_P T}{P} \left( \frac{d \ln T}{d \ln P} - \nabla_{\rm ad} \right), \qquad (2)$$

where $c_P = T(\partial s/\partial T)_P$ is the specific heat at constant pressure and $\nabla_{\rm ad} = (\partial \ln T/\partial \ln P)_s$. The entropy advection is given by how much the temperature gradient differs from the adiabat. In the static state, the gradient of the luminosity itself is then

$$\frac{dL}{dP} = \langle \dot{M} \rangle c_P \left[ \frac{dT}{dP} - \left( \frac{\partial T}{\partial P} \right)_s \right] - \frac{4\pi r^2 \epsilon_N}{g}, \qquad (3)$$

which we use with the equations for heat transport and hydrostatic equilibrium to solve for both the structure and luminosity in the envelope, resulting in values of $L$ and $L_{\rm core}$ that depend on values of $T_c$, $M$, $\langle \dot{M} \rangle$, and $M_{\rm acc}$. The contribution to $L$ from accretion is the heat not advected with the material and is referred to in the literature as "compressional heating." Although this choice of words is unfortunate since the action occurring is more like cooling, we use this common term in our discussions. In all the calculations presented here we use a fixed $R$ for the last term in equation (3), that of a zero temperature WD: 8.8, 5.7, and $4.1 \times 10^8$ cm for $M = 0.6$, 1.0, and 1.2 $M_\odot$, respectively. As a single point check, matching the bottom of the envelope and the outer edge of a finite-temperature core model yields $R = 8.9 \times 10^8$ cm for $M = 0.6\ M_\odot$, $\langle \dot{M} \rangle = 6 \times 10^{-11}\ M_\odot\ {\rm yr}^{-1}$, and $M_{\rm acc} = 1.4 \times 10^{-4}\ M_\odot$. By dropping the nuclear burning term and making a few other simplifying assumptions, equation (3) can be integrated analytically to obtain an approximate luminosity $L \approx 3\langle \dot{M} \rangle kT_c/\mu m_p$ (see Appendix B), where $k$ is Boltzmann's constant, $m_p$ is the proton mass, and $\mu \simeq 0.6$ is the mean molecular weight of the freshly accreted envelope.

Since $M_{\rm acc}$ changes with time as $M_{\rm acc}(t) = \langle \dot{M} \rangle \Delta t$, the static envelope structure is an approximation to the evolution. For this method to be accurate, we want the neglected term to be small, namely, $|\partial s/\partial t| \ll |v_r\, \partial s/\partial r|$. Evaluating at a fixed pressure and using equation (2) gives

$$\left| \frac{\partial T}{\partial t} \right| \ll \frac{T}{\tau_{\rm acc}} \left| \nabla_{\rm ad} - \frac{d \ln T}{d \ln P} \right|, \qquad (4)$$

where $\tau_{\rm acc} = P/g\dot{m}$ is the accretion time. Dropping the temperature gradient (good in the conductive regions), finite differencing, and setting $\Delta t = \tau_{\rm acc}$ leads to the condition $\Delta T/T \ll 2/5$, where $\Delta T$ is the temperature change at the envelope base during accumulation. As will be shown in § 4, the evolution of $M_{\rm acc}$ takes place at constant $T_c$, so this condition is always satisfied and our static structures are an excellent approximation for the accumulating envelope.

Now we wish to consider the effect of the outer boundary condition on the structure of the envelope. To determine this we compare the thermal cooling time of an outer layer, $\tau_{\rm th} = \Delta M c_P T/L$, to the time to accrete that layer, $\tau_{\rm acc} = \Delta M/\langle \dot{M} \rangle$. Here $\Delta M$ is the mass of the (thin) outer layer being considered, $T$ is the temperature of the layer, and $L$ is the overall luminosity, which is driven mostly by energy released from deeper layers, $L \approx c_p \langle \dot{M} \rangle T_c$. Thus the ratio $\tau_{\rm th}/\tau_{\rm acc} \approx T/Tc$, so that where $T \ll T_c$ in the outer layers, the material can cool much more quickly than it is being accreted and therefore has no influence over the thermal structure of deeper layers. In other words, the entropy of the outer envelope is determined by the luminosity flowing through it rather than by any external boundary condition. The condition $T \ll T_c$ is sometimes violated during a DN event, where either the high external radiation field (Pringle 1988) or the more rapid accretion (Sion 1995; Godon & Sion 2002) temporarily modifies the outermost layers of the WD envelope. However, this heat does not penetrate to depths critical for the WD core but only to a depth where the thermal time is of order the duration of the DN outburst and is the likely cause of the fading $T_{\rm eff}$ seen following a DN outburst (see Sion 1999 for a review).

In addition to the downward motion due to accretion, the heavier helium ions will sink with respect to the overall flow. While we have not included this effect, we estimate here when it is important. The drift velocity of the He ions is $v_{\rm drift} \simeq 2m_p gD/kT$, where $D$ is the thermal diffusion coefficient (see Deloye & Bildsten 2002). This is to be compared with the downward velocity of the fluid due to accretion, $v_{\rm acc} = \langle \dot{M} \rangle / 4\pi R^2 \rho$. In the simplest approximation, Coulomb scattering off protons dominates and $D = 0.024 \Lambda^{-1} T_7^{5/2} \rho_4^{-1}$ cm$^2$ s$^{-1}$ (Alcock & Illarionov 1980), where $T_7 = T/10^7$ K, $\rho_4 = \rho/10^4$ g cm$^{-3}$, and $\Lambda$ is the Coulomb logarithm. For $v_{\rm drift} < v_{\rm acc}$ this yields the relationship $\langle \dot{M} \rangle > 10^{-11}\ M_\odot\ {\rm yr}^{-1} T_7^{3/2} (M/0.6\ M_\odot) \Lambda^{-1}$, so that for our lowest accretion rate, $10^{-11}\ M_\odot\ {\rm yr}^{-1}$, where $T_7 = 0.4$, only the high-mass models deserve further scrutiny. Below this accretion rate, the energy release due to sedimentation of the helium in the accreted material can be a moderate fraction of that released due to compression. For our $M = 1.0\ M_\odot$ model with $\langle \dot{M} \rangle = 10^{-11}\ M_\odot\ {\rm yr}^{-1}$, the conditions at the base of the H/He layer when $M_{\rm acc} = 0.90 M_{\rm ign}$ are $\rho = 1.4 \times 10^4$ g cm$^{-3}$ and $T = 4.1 \times 10^6$ K, so that the Coulomb coupling parameter $\Gamma = 2$. Diffusion coefficients in this gas-liquid crossover regime have yet to be authoritatively calculated. Using the fitting form of Iben & MacDonald (1985), which is very similar to the canonical results of Paquette et al. (1986) in this regime (See Iben, Fujimoto, & MacDonald 1992b), we obtain $v_{\rm drift}/v_{\rm acc} = 1.3$. However, using the liquid diffusion results of Wallenborn & Baus (1978), we obtain $v_{\rm drift}/v_{\rm acc} = 0.38$. Regardless of this uncertainty, it is clear that in future work diffusion needs to be considered for $M \geq 1.0\ M_\odot$ and $\langle \dot{M} \rangle \leq 10^{-11}\ M_\odot\ {\rm yr}^{-1}$. As inferred from the amount of sedimentation found by Iben et al. (1992b), this limit is at a higher value of $\langle \dot{M} \rangle$ when a higher value of $T_c$ is assumed.

### 2.2. *Accreting Envelope*

We now present results from the envelope models, investigating how $\langle \dot{M} \rangle$ and $M_{\rm acc}$ determine the $L$-$T_c$ relationship. The outer boundary is at $P = 10^{10}$ ergs cm$^{-3}$ in the upper edge of the radiative layers. We set the temperature there to that of a radiative zero solution for $L = 4\pi R^2 \sigma_{\rm SB} T_{\rm eff}^4$. Then equation (3) and the other structure equations are integrated inward, keeping track of $L(P)$ and $T(P)$, to $P = gM_{\rm acc}/4\pi R^2$, the base of the accreted layer. Interior to this, $L = L_{\rm core}$ is taken to be constant and the integration is continued, using a pure carbon composition for simplicity, until $P = 40P_{\rm ign}$, where $P_{\rm ign} = gM_{\rm ign}/4\pi R^2$ and $M_{\rm ign}$ is found consistently at each value of $\langle \dot{M} \rangle$. A value of $P = 2 \times 10^{20}$ ergs cm$^{-3}$ is used for the $M = 0.6\ M_\odot$ demonstrations in this section, corresponding to the $M_{\rm ign}$ value for an equilibrated model at $\langle \dot{M} \rangle = 10^{-10}\ M_\odot$ yr$^{-1}$. We label the temperature at the point where we stop the integration "$T_c$," interior to which the core is isothermal. The equation of state for the electrons and ions was taken from analytical approximations of Paczyński (1983), with Coulomb corrections from Farouki & Hamaguchi (1993). The radiative opacities from OPAL (Iglesias & Rogers 1996) and the conductivities of Itoh et al. (1983) were used. Nuclear reaction rates and energies are from Caughlan & Fowler (1988), with screening enhancement factors for high density from Ichimaru (1993), which also appear in Ogata, Iyetomi, & Ichimaru (1991).

The above treatment of the outer edge of the C/O core provides a reasonable approximation to the evolution of this region during a CN cycle without the complications of explicit simulation. At $40P_{\rm ign}$ the temperature change due to adiabatic compression is 1%. Under this approximation in the equilibrium state discussed in § 4, fluid elements near the base of the accreted layer move on paths for which they must lose entropy during the CN cycle, i.e., ones more shallow than the adiabat in the $T$-$P$ plane. Deeper fluid elements move on paths for which they must gain entropy, steeper than the adiabat. This exchange is consistent with our expectation for the actual evolution, and since it only contributes peripherally by setting the gross temperature excursion from $T_c$ at the base of the accreted layer, the accuracy of a more sophisticated treatment is not considered worth its price in complexity at this point. The fraction of the core affected by the CN cycle in this treatment is also roughly consistent with that expected on energetic grounds. For example, a luminosity of $10^{-3}\ L_\odot$ delivers enough energy in the interval between CNs, $\sim 10^6$ yr, to raise the temperature of the outer $10^{-3}\ M_\odot$ of the core by $10^6$ K ( $\sim$10%); this mass coordinate corresponds to a pressure of just under $10^{20}$ ergs cm$^{-3}$.

The relationship between $L$ and $T_c$ for several values of $\langle \dot{M} \rangle$ are shown in Figure 1 for a 0.6 $M_\odot$ WD ($R = 8.76 \times 10^8$ cm) with $M_{\rm acc} = 5 \times 10^{-5}\ M_\odot$. This $M_{\rm acc}$ value is less than the CN ignition mass for most of the range of $\langle \dot{M} \rangle$ values and is comparable to the hydrogen layers on cooling WDs. All the demonstration curves in this section are for $X_{^3{\rm He}} = 0.001$. Shown for reference (*dotted line*) is the $L$-$T_c$ relation for an isolated 0.6 $M_\odot$ WD with pure layers of mass $M_{\rm H} = 6 \times 10^{-5}\ M_\odot$ and $M_{\rm He} = 6 \times 10^{-3}\ M_\odot$ (Hansen 1999). The corresponding relation for our envelope model, with $\langle \dot{M} \rangle = 0$, is shown as the dashed line and provides an initial comparison to previous work. The offset from the cooling WD is due to the H/He envelope being more opaque than that of pure hydrogen. The slightly larger divergence for $10^7\ {\rm K} < T_c < 2 \times 10^7$ K is likely due to the radiative-conductive transition point lying below the outer H-rich layer, a location where the cooling model has a thick layer of helium, whereas our envelope is pure carbon. The sharp change in the dotted line at $L < 10^{-4}\ L_\odot$ is due to surface convection extending down into the conductive regions, commonly termed "convective coupling" (Fontaine et al. 2001). To avoid this complication, we have restricted ourselves to $L > 10^{-4}\ L_\odot$, where the outer convective layer need not be modeled directly to determine the $L$-$T_c$ relation.

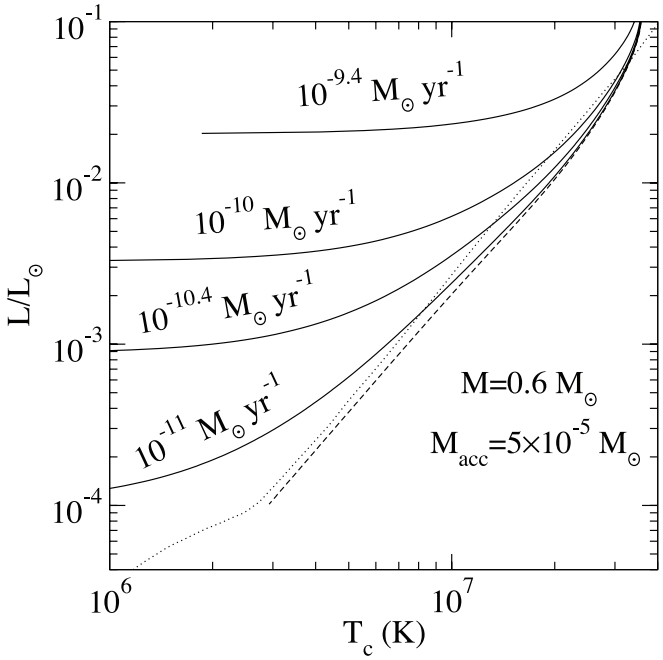


FIG. 1.—Exiting surface luminosity $L$ as a function of core temperature $T_c$ for a 0.6 $M_\odot$ WD. The accumulated H/He layer has a mass $M_{\rm acc} = 5 \times 10^{-5}\ M_\odot$. Various accretion rates are shown as labeled solid lines with $\langle \dot{M} \rangle = 10^{-11}$, $10^{-10.4}$, $10^{-10}$, and $10^{-9.4}\ M_\odot$ yr$^{-1}$. The dashed line has $\langle \dot{M} \rangle = 0$, and the dotted line is the $L$-$T_c$ relation of an isolated cooling DA WD with pure layers of mass $M_{\rm H} = 6 \times 10^{-5}\ M_\odot$ and $M_{\rm He} = 6 \times 10^{-3}\ M_\odot$ (Hansen 1999).

### 2.3. *Parameter Dependences of White Dwarf Luminosities*

We now discuss how the $L$-$T_c$ relation changes under active accretion. It is only for low values of $\langle \dot{M} \rangle$ and high values of $T_c$ that the luminosity flowing through the envelope is dominated by the hot core. The value of $T_c$ below which the energy release due to accretion becomes important is determined by $\langle \dot{M} \rangle$; higher values release energy faster via compressional heating and therefore their luminosity becomes dominated by accretion at a higher value of $T_c$. Thus in Figure 1, while there is a large area of the curve at $\langle \dot{M} \rangle = 10^{-11}\ M_\odot$ yr$^{-1}$ for which core cooling dominates at this value of $M_{\rm acc}$, there is little such area at $\langle \dot{M} \rangle = 10^{-9.4}\ M_\odot$ yr$^{-1}$. The upturn in the luminosity at $T_c \gtrsim 3 \times 10^7$ K is due to energy released from fusion of $^3$He, a species not present in abundance in the cooling models. The onset of the nuclear energy source is quite sensitive to $M_{\rm acc}$ since the conditions ($T$, $\rho$) at the base of the H/He layer dominate this effect (see § 3 for details).

The other major feature of the $L$-$T_c$ curve is the minimum value of $L$ for a given $\langle \dot{M} \rangle$. In this situation the envelope determines its own temperature and the surface luminosity becomes independent of $T_c$. There is a temperature inversion in the envelope: the temperature rises inward through the

radiative layer, flattens out when conduction becomes dominant, passes through a value $T_{\rm max}$, and then decreases toward the core. The energy liberated by compression goes into the core as well as coming out the surface. This lower limit, $L(T_c \rightarrow 0)$, is shown in Figure 2 as a function of $\langle \dot{M} \rangle$. The upper solid curve is for $M = 0.6\ M_\odot$ and $M_{\rm acc} = 5 \times 10^{-5}\ M_\odot$. Raising $M_{\rm acc}$ does not change the relation—a curve for $M_{\rm acc} = 10^{-4}\ M_\odot$ is indistinguishable—except to reduce the maximum $L$ at which such a self-supported envelope state can exist. A higher $M_{\rm acc}$ leads to a higher density at the base of the accreted layer and causes fusion to become important at lower envelope temperatures and luminosities.

The dotted line is a rough approximation found by identifying $T_{\rm max}$ with the core temperature of a cooling WD, giving $L \propto T_{\rm max}^{2.5} M$, and by assuming that those losses are matched by compressional heating, so that $L \approx 3\langle \dot{M} \rangle k T_{\rm max}/\mu m_p$ (from Appendix B). Putting these together and using the point at $\langle \dot{M} \rangle = 10^{-11}\ M_\odot\ {\rm yr}^{-1}$ to set the constant gives $L(\langle \dot{M} \rangle) = 1.08 \times 10^{-4}\ L_\odot (\langle \dot{M} \rangle / 10^{-11}\ M_\odot\ {\rm yr}^{-1})^{5/3} (M/0.6\ M_\odot)^{-2/3}$ (*dotted line*). Calibrating the cooling luminosity separately from the $\langle \dot{M} \rangle = 0$ curve in Figure 1 gives a prefactor that differs from this by less than a factor of 2, demonstrating that the estimate from Appendix B is good for low values of $\langle \dot{M} \rangle$. While the $L \propto \langle \dot{M} \rangle^{5/3}$ dependence is fairly well matched at low values of $\langle \dot{M} \rangle$, the full calculation gives increasingly lower luminosities at higher values of $\langle \dot{M} \rangle$ because when fusion provides some of the energy, $T_{\rm max}$ need not be as high, so the luminosity is less. The lower solid line gives $L(T_c \rightarrow 0)$ for $M = 1.0\ M_\odot$ and is fairly consistent with $(1.0/0.6)^{-2/3}$ times the $M = 0.6\ M_\odot$ curve, shown as the dashed line. The $M = 1.0\ M_\odot$ curve follows $L \propto \langle \dot{M} \rangle^{5/3}$ to higher values of $\langle \dot{M} \rangle$ than that for $M = 0.6\ M_\odot$.

Finally, we explore the dependence of the $L$-$T_c$ relation on $M_{\rm acc}$. Generally, the energy released by compression in the envelope should increase with $M_{\rm acc}$ because of the lower value of $\mu$ for H/He relative to C/O as it appears in the compressional heating term (see eq. [3]). Energy from hydrogen fusion should also increase with $M_{\rm acc}$. The upper curves in Figure 3 show $L$ for $M_{\rm acc}$ values of 0.5, 1, 3, and $5 \times 10^{-4}\ M_\odot$ for a $0.6\ M_\odot$ WD accreting at $\langle \dot{M} \rangle = 10^{-10.4}\ M_\odot\ {\rm yr}^{-1}$. This accretion rate, $\approx 4 \times 10^{-10}\ M_\odot\ {\rm yr}^{-1}$, is characteristic of gravitational-wave–driven accretion for DNs below the period gap (Kolb & Baraffe 1999). Also shown for comparison is $\langle \dot{M} \rangle = 10^{-11}\ M_\odot\ {\rm yr}^{-1}$. As $M_{\rm acc}$ is increased from 0.5 to $1 \times 10^{-4}\ M_\odot$, three important features are apparent. At $T_c \lesssim 3 \times 10^6$ K the exiting surface luminosity $L$ is nearly unchanged because the additional energy released in the envelope is transported into the core with a negligible rise in $T_{\rm max}$. For $3 \times 10^6\ {\rm K} \lesssim T_c \lesssim 10^7$ K, $T_c$ is high enough that the additional compressional heating energy is forced outward and acts as an additive factor on top of the cooling luminosity, and there is a small increase across this range. At $T_c \gtrsim 1.5 \times 10^7$ K, the density has become high enough that the large amount of energy released by fusion has destabilized the envelope at these temperatures. This is discussed further in § 3.

The crossover behavior in $T_c$ between core heating at low values of $T_c$ and cooling at higher values can be seen directly in Figure 4, which shows $L_{\rm core}$, the luminosity exiting the core into the base of the accreted layer. In order to maintain a logarithmic scale, two panels are displayed: the top one displays positive $L_{\rm core}$ values and therefore core cooling, and the bottom one displays negative $L_{\rm core}$ values to show core heating. When increasing $M_{\rm acc}$ from 0.5 to $1 \times 10^{-4}\ M_\odot$ (*solid and dashed curves, respectively*) the core heating increases at $T_c \lesssim 4 \times 10^6$ K. The core cooling, present at higher temperatures, remains fixed with this $M_{\rm acc}$ increase; the additional compressional heating is increasing $L$. Note that at a single $T_c \simeq 4$–$5 \times 10^6$ K,

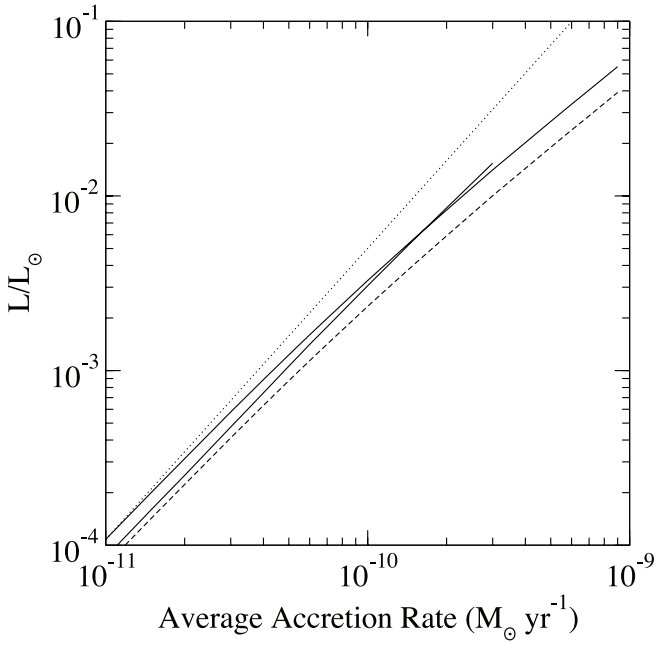


FIG. 2.—Surface luminosity as a function of $\langle \dot{M} \rangle$ for very cold WD cores. The upper solid line is for $M = 0.6\ M_\odot$ and the lower solid line is for $M = 1.0\ M_\odot$, both with $M_{\rm acc} = 5 \times 10^{-5}\ M_\odot$. The dashed line shows the values for the top solid line scaled by $(1.0/0.6)^{-2/3}$ in order to demonstrate that our analytic WD mass dependence is close to correct. The dotted line is the analytical approximation discussed in the text.

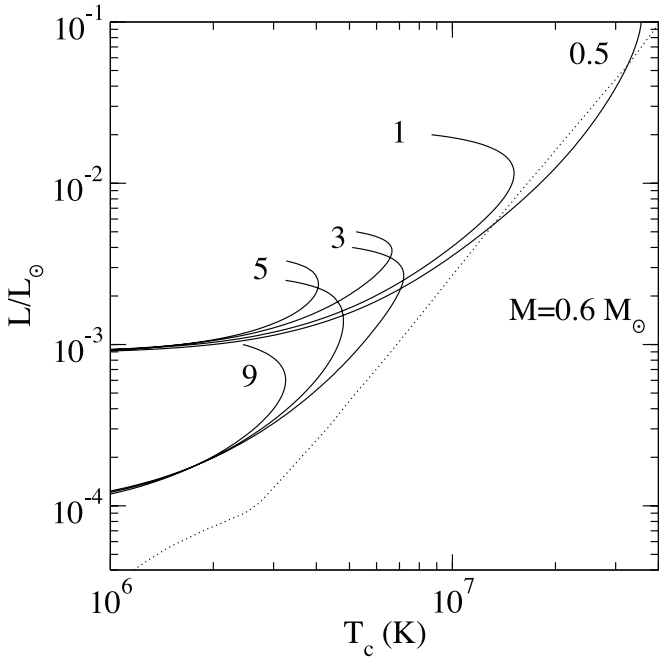


FIG. 3.—WD surface luminosity $L$ as a function of $T_c$ for various accumulated layer masses. The upper set of solid lines all have $\langle \dot{M} \rangle = 10^{-10.4}\ M_\odot\ {\rm yr}^{-1}$ and $M_{\rm acc} = 0.5, 1, 3,$ and $5 \times 10^{-4}\ M_\odot$ as indicated. The lower set of solid lines has $\langle \dot{M} \rangle = 10^{-11}\ M_\odot\ {\rm yr}^{-1}$ and $M_{\rm acc} = 3, 5,$ and $9 \times 10^{-4}\ M_\odot$. The WD mass is $0.6\ M_\odot$ for all cases. The dotted line is the $L$-$T_c$ relation of an isolated cooling DA WD with pure layers of mass $M_{\rm H} = 6 \times 10^{-5}\ M_\odot$ and $M_{\rm He} = 6 \times 10^{-3}\ M_\odot$ (Hansen 1999).

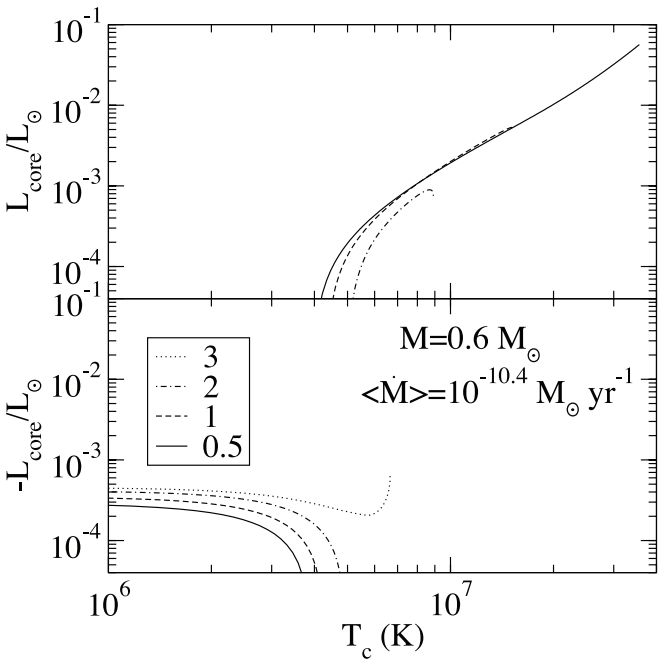


FIG. 4.—Luminosity $L_{\rm core}$ entering the accreted layer from the core below as a function of $T_c$ for various accumulated layer masses $M_{\rm acc}$ on a 0.6 $M_\odot$ WD. The top panel shows the rate of core cooling ($L_{\rm core}$) and the bottom the rate of heating ($-L_{\rm core}$). The accretion rate is set at $\langle \dot{M} \rangle = 10^{-10.4}\ M_\odot\ {\rm yr}^{-1}$, and $M_{\rm acc}$ takes values of 0.5, 1, 3, and $5\times10^{-4}\ M_\odot$ as indicated. For clarity the curves have been truncated at the turning point seen at high values of $T_c$ in Fig. 3.

both core-heating and core-cooling envelope states are available, depending on the value of $M_{\rm acc}$.

Our survey of parameters is now complete, and in § 4 we use $L_{\rm core}$ to discuss the thermal evolution of the C/O core. Of the parameters discussed, $\langle \dot{M} \rangle$ will be an independent variable while $T_c$ will be found from $\langle \dot{M} \rangle$ and $M$. However, $M_{\rm acc}$ has a maximum value set by the stability of the envelope, which we now discuss.

## 3. CALCULATING THE IGNITION MASS

The accreted mass $M_{\rm acc}$ increases until a thermonuclear instability causes a CN explosion at $M_{\rm acc} = M_{\rm ign}$, which depends principally on the temperature in the accreted layer. There are two ignition modes: (1) a traditional thin-shell instability created by the temperature sensitivity of thermonuclear reactions and (2) a global instability of the envelope relevant when $\kappa_{\rm cond} \ll \kappa_{\rm f\text{-}f}$ ($T \lesssim 8 \times 10^6$ K here). The mode giving the lower value of $M_{\rm ign}$ is the active mode, and each is elaborated below.

The instability manifests in the $L$-$T_c$ relation as a turning point, or a maximum $T_c$ as a function of $L$, as seen earlier in Figure 3. A general discussion of the relationship between turning points and stability in thin-shell accretion appears in Paczyński (1983). Because of the large heat capacity of the core and the choice of the lower boundary as described in § 2.2, $T_c$ is essentially constant while $M_{\rm acc}$ increases and the turning point moves to lower temperatures. If we define $M_{\rm ign}(T_c)$ to be the value of $M_{\rm acc}$ at which the turning point happens at $T_c$, the envelope structures with $M_{\rm acc} < M_{\rm ign}(T_c)$ form a connected quasi-static sequence at constant $T_c$ terminating at $M_{\rm ign}$. Evolution forward in time from this envelope state must be followed in a fully time-dependent fashion rather than quasi-statically, and so we consider this terminus the ignition point of the CN explosion. The envelope is assumed to have switched to a "high," burning state, about which we will make two assumptions: (1) it is short-lived and therefore of small thermal importance to the core, and (2) during it, most or all of the accreted material is ejected. The thick solid curves in Figure 5 show the conditions at the base of the accreted layer at ignition for the models equilibrated in the manner discussed in § 4 for two values of $M$. Two values of $X_{^3{\rm He}}$ are shown at each $M$, representing the range expected in CVs.

The lower dot-dashed line in Figure 5 gives the division between radiative and conductive heat transport, where $\kappa_{\rm f\text{-}f} = \kappa_{\rm cond}$. Above this line radiation dominates the heat transfer at the base of the accreted layer and the instability is well predicted by a traditional thin-shell instability criterion. Since the scale height of the envelope $h = P/\rho g \ll R$, it has a positive heat capacity and is therefore subject to a thermal instability that occurs when the inequality

$$\left(\frac{\partial \epsilon_{\rm cool}}{\partial T}\right)_P < \left(\frac{\partial \epsilon_{\rm nuc}}{\partial T}\right)_P \tag{5}$$

is satisfied at the base of the accreted material. Here $\epsilon_{\rm nuc}$ is the energy generated by the fast component of nuclear burning; the important chains are $^{12}{\rm C}(p,\gamma)^{13}{\rm N}$ (the first step of CNO), $^{1}{\rm H}(p,\beta^+\nu){\rm D}(p,\gamma)^{3}{\rm He}$ (the first two steps of the $p$-$p$ chains), $^{3}{\rm He}(^{3}{\rm He},2p)^{4}{\rm He}$, and $^{3}{\rm He}(\alpha,\gamma)^{7}{\rm Be}(e^-,\nu)^{7}{\rm Li}(p,\alpha)^{4}{\rm He}$ (Clayton 1983). To represent local cooling due to heat transfer, we define

$$\epsilon_{\rm cool} \equiv \frac{g^2}{P^2}\frac{4acT^4}{3\kappa}\ , \tag{6}$$

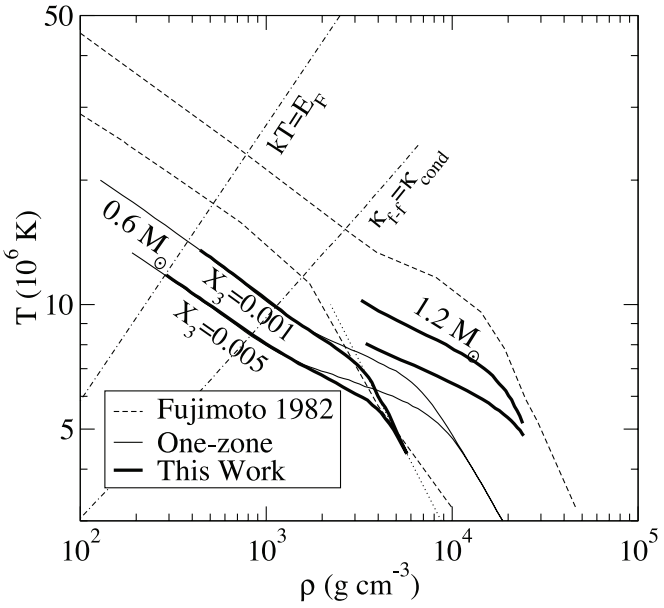


FIG. 5.—Conditions at the base of the H/He accreted layer at ignition of a CN for $M = 0.6\ M_\odot$ and $M = 1.2\ M_\odot$. The thin solid curves are the local condition given by eq. (5), the dotted curves are the global ignition condition given by $L_\odot(T_b/10^8\ {\rm K})^{2.5}(M/0.6\ M_\odot) = M_{\rm ign}\epsilon_N(\rho_b, T_b)$, and the thick curves are the actual conditions found for equilibrated models. The dashed lines are the base conditions from ignition calculations by Fujimoto (1982).

reflecting the rate at which a thermal perturbation on the size of the pressure scale height $h$ damps out. The use of division by the scale height in lieu of a derivative to form $\epsilon_{\rm cool}$ is commonly termed a "one-zone approximation." See Paczyński (1983) for an in-depth example. Equation (5) further approximates that the pressure response to a small temperature perturbation is negligible, a good approximation when $h \ll R$. This ignition condition is identical to that used by Fujimoto, Hanawa, & Miyaji (1981) to study X-ray bursts, although our notation is somewhat different. When the inequality of equation (5) is satisfied, thermal perturbations will grow since there is not sufficient cooling to halt the nuclear runaway. We evaluate the derivatives using our full equation of state and $\kappa$ to obtain a maximum temperature at a given density for the base of H/He layer, shown as the thin solid curves in Figure 5 for the two values of $X_{^3\rm He}$. When the base temperature in the H/He layer exceeds this value, ignition occurs. This agrees with the location of the turning point in the $L$-$T_c$ relations in the radiative regime (see Fig. 3).

In the radiative regime the opacity is due to free-free absorption, and at moderate temperatures the triggering nuclear reaction is $^3$He + $^3$He fusion. Both the heating and the cooling can be well approximated by power laws, so that the ignition condition can be written in closed form. Expanding $\epsilon_{\rm nuc}$ about $T = 10^7$ K and using an ideal-gas equation of state, equation (5) becomes

$$\rho_{\rm ign} \gtrsim 1.2 \times 10^3 \text{ g cm}^{-3} T_7^{-3.21} \left(\frac{X_3}{0.001}\right)^{-1/2} g_8^{1/2}, \quad (7)$$

where $T_7 = T/10^7$ K and $g_8 = g/10^8$ cm s$^{-2}$, matching the radiative portion of the curves shown in Figure 5.

When the base of the envelope becomes degenerate, i.e., when $\kappa_{\rm cond} \ll \kappa_{\rm f\text{-}f}$, the turning point happens at a lower value of $M_{\rm acc}$ than the one-zone model predicts, as shown by the divergence of the thick lines in Figure 5 from the thin lines of the one-zone prediction. The second ignition mode has become important and involves an interaction between the radiative and conductive regions in the envelope. In order to clarify the envelope state in this global ignition mode, we now present how this maximum $T_c$ arises from a simple analytical model when the base of the accreted layer is in the conductive region. Define $T_b$ as the temperature at the base of the accreted layer; the location of the point of transition to conduction at the bottom of the radiative layer leads to $L = L_0 (T_b/T_0)^{2.5}$, where $L_0$ and $T_0$ are fiducial parameters. Using a coefficient $K_b$ to characterize the thermal conduction, the heat coming from the core is $L_{\rm core} = K_b (T_c - T_b)/z_{bc}$, where $z_{bc}$ is the distance below the base of the accreted layer at which $T = T_c$ and we ignore the dependence of $K$ on temperature and density. If the nuclear heating during accumulation is approximated by $L_N = \epsilon_N(\rho_b, T_b) M_{\rm acc}$, where $\rho_b$ is the density at the base of the accreted layer derived from $P_b = g M_{\rm ign}/4\pi R^2$, these quantities are related by $L = L_{\rm core} + L_N$, neglecting compressional heating, or

$$T_c \simeq T_0 \left(\frac{L}{L_0}\right)^{0.4} + \frac{z_{bc}}{K} \times \left[L - M_{\rm acc}\epsilon_N|_{7\times10^6\rm K} \left(\frac{T_0}{7\times10^6 \text{ K}}\right)^{5.2} \left(\frac{L}{L_0}\right)^{2.1}\right]. \quad (8)$$

Here we have taken $T_b = T_0 (L/L_0)^{1/2.5}$ and expanded $\epsilon_N$ about $T = 7 \times 10^6$ K so as to quantify the temperature dependence of the burning rate in the regime of interest; only the $p + p \rightarrow {}^3$He reaction chain is included at this low temperature. For low luminosities, $T_c$ increases with $L$, but eventually the nuclear heating becomes strong enough that a maximum $T_c$ is reached. With the outer temperature boundary of the conductive region set by the radiative-conductive transition and the inner temperature boundary fixed by the thermal inertia of the core, the heat released by nuclear processes cannot be transported out of the conductive region and therefore builds up rapidly, leading to an explosion.

A simple approximation of the maximum of equation (8) is obtained by finding when the opposing terms $L$ and $M_{\rm acc}\epsilon_N$ are comparable. This gives the simple form $L_0 (T_b/T_0)^{2.5} (M/0.6\ M_\odot) = M_{\rm ign}\epsilon_N(\rho_b, T_b)$. This expresses that $M_{\rm ign}$ is the accumulated mass for which the outgoing luminosity is wholly provided by nuclear burning, giving a maximal envelope state before CN runaway. By expanding $\epsilon_N$ at the lowest $T$ point of the solid line for $M = 0.6\ M_\odot$, $T = 4.36 \times 10^6$ K, and $\rho = 5.7 \times 10^3$ g cm$^{-3}$, using only the $p$-$p$ reaction as above but including the screening correction, we obtain $\epsilon_N \propto T^{5.73}\rho^{1.17}$. The dotted line shown in Figure 5 is this form with the prefactor adjusted to fit the lowest temperature point of our actual envelope calculation for $M = 0.6\ M_\odot$ (*lower thick solid lines*). Using an $L$-$T_b$ relation fitted to the $\langle \dot{M} \rangle = 0$ line in Figure 1 gives a result that is parallel and only a factor of 2 lower in density, mostly because of neglecting the inward-bound heat from the dropped term.

The dashed lines in Figure 5 give the results found by Fujimoto (1982) for $M = 0.6\ M_\odot$ (*lower line*) and $1.2\ M_\odot$ (*upper line*). Our results are consistent with these in the demonstration of two ignition modes. The largest difference is due to our inclusion of $^3$He in the accreted matter as a nuclear energy source. Our calculation of ignition with $X_3 = 0$ is roughly 5% higher in temperature than that of Fujimoto (1982) in the radiation-transport–dominated regime. Much of this 5% discrepancy is likely from our updated opacities.

## 4. THE THERMAL EQUILIBRIUM OF THE WHITE DWARF CORE

Section 2 introduced the envelope models that provide $L(M_{\rm acc}, \langle \dot{M} \rangle, T_c, M)$. These same models also provide $L_{\rm core}(M_{\rm acc}, \langle \dot{M} \rangle, T_c, M)$, the luminosity passing through the base of the envelope from the core. The variation of $L_{\rm core}$ with $M_{\rm acc}$ at several values of $T_c$ and two accretion rates is shown in Figure 6. Each of these curves extend in $M_{\rm acc}$ to the CN ignition[1] and make clear the amount of heat exchanged between the envelope and the WD core over the CN cycle, with core cooling occurring at low values of $M_{\rm acc}$ and core heating at high values. This allows us to calculate an equilibrium core temperature $T_{c,\rm eq}$, where the heating and cooling of the core are equal over the CN cycle (Townsley & Bildsten 2002). At the onset of accretion in the binary, the WD core has $T_c < T_{c,\rm eq}$ and is heated during the CN cycle. We now find the time it takes to reach $T_{c,\rm eq}$ at a given value of $\langle \dot{M} \rangle$.

At low values of $\langle \dot{M} \rangle$ any long-term compression (expansion) of the WD core due to mass gain (loss) has little impact on the envelope (see Appendix A). Hence, for simplicity, we assume that the accumulated mass is ejected in a CN, keeping

[1] The CN explosion has a negligible effect on the thermal content of the core because of its short duration compared to the envelope accumulation time.

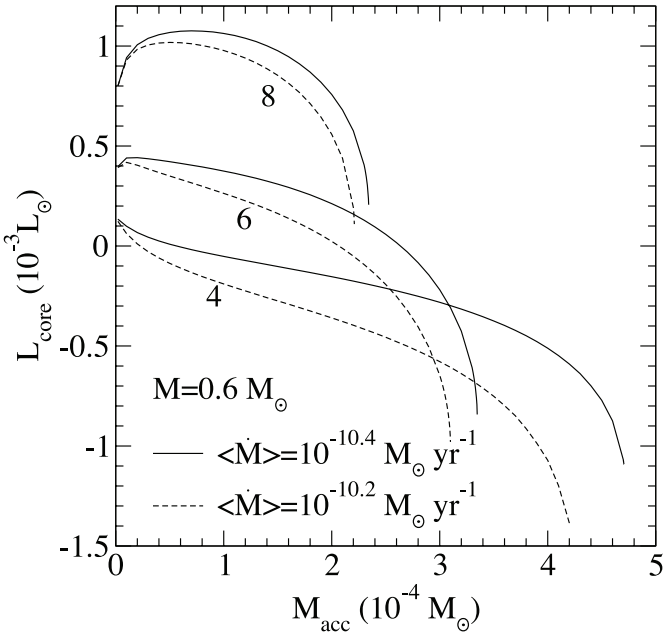


FIG. 6.—Luminosity exiting the WD core as a function of $M_{\rm acc}$ for several values of $T_c$ as indicated in units of $10^6$ K. All curves have $M = 0.6\ M_\odot$; the solid curves have $\langle \dot{M} \rangle = 10^{-10.4}\ M_\odot\ {\rm yr}^{-1}$, while the dashed ones have $\langle \dot{M} \rangle = 10^{-10.2}\ M_\odot\ {\rm yr}^{-1}$.

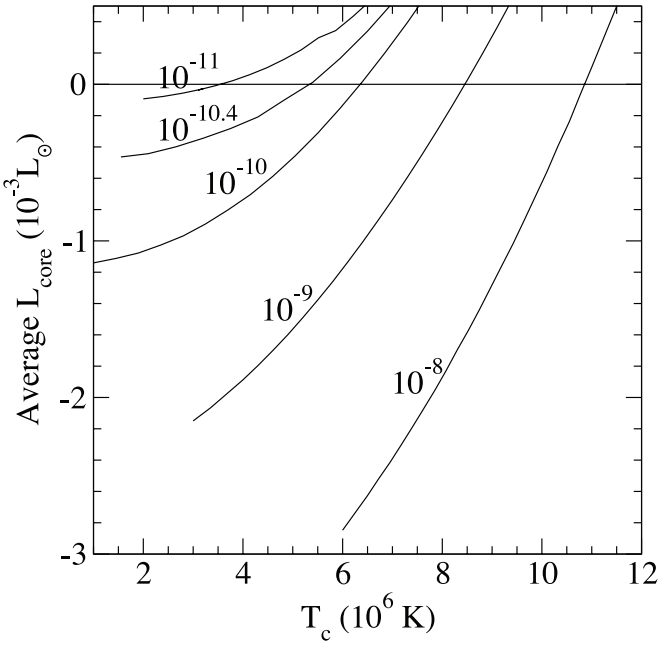


FIG. 7.—Time-averaged luminosity escaping from the core during the accretion of matter up to a CN event. The curves have $\langle \dot{M} \rangle$ as indicated in units of $M_\odot\ {\rm yr}^{-1}$, and $M_{\rm WD} = 0.6\ M_\odot$.

$M$ constant. We begin by defining an average core heating rate presuming that $M$ and $T_c$ are constant while $M_{\rm acc}$ changes,

$$\langle L_{\rm core} \rangle (\langle \dot{M} \rangle, T_c, M) = \frac{1}{t_{\rm CN}} \int_0^{t_{\rm CN}} L_{\rm core}\left[M_{\rm acc}(t), \langle \dot{M} \rangle, T_c, M\right] dt\,. \tag{9}$$

Using this $\langle L_{\rm core} \rangle$ to make statements about the WD's evolution implicitly assumes that the star's only memory of the CN cycle is the net heat gained or lost during it; otherwise, it returns to a state identical to that at the same stage in the previous cycle. Figure 7 shows the dependence of $\langle L_{\rm core} \rangle$ on $T_c$ for several accretion rates. We find that $\langle L_{\rm core} \rangle$ increases with $T_c$ from two effects: (1) the cooling luminosity is greater at higher values of $T_c$, causing stronger core cooling for small values of $M_{\rm acc}$, and (2) the maximum $M_{\rm acc}$ is larger at lower values of $T_c$, allowing for a longer period of core heating when $M_{\rm acc}$ is large. The equilibrium point where $\langle L_{\rm core} \rangle = 0$ for $M = 0.6\ M_\odot$ and $\langle \dot{M} \rangle = 10^{-10.4}\ M_\odot\ {\rm yr}^{-1}$ is $T_c \approx 5.5 \times 10^6$ K. For $T_c \approx T_{c,{\rm eq}}$, the envelope transitions from a state that allows the core to cool at low values of $M_{\rm acc}$ to a state that heats the core at high values. The positive slope of $\langle L_{\rm core} \rangle$ at $T_c \approx T_{c,{\rm eq}}$ implies that the equilibrium state is stable; i.e., a higher value of $T_c$ at the same value of $\langle \dot{M} \rangle$ causes the core to radiate and lower its temperature. The figure also makes clear that $T_{c,{\rm eq}}$ increases with $\langle \dot{M} \rangle$ in order to maintain equilibrium under the additional heat deposition.

The specific heat of the liquid WD core is $\approx 3k/\mu_i m_p$, where $\mu_i \approx 14$ is the ion mean molecular weight (see Appendix A). When $T_c < T_{c,{\rm eq}}$, the core is heated by the envelope at the rate shown in Figure 7, allowing for a simple integration of

$$\langle L_{\rm core} \rangle \approx -\frac{3kM}{\mu_i m_p} \frac{dT_c}{dt}\,, \tag{10}$$

to yield the time to reach the equilibrium. For a comparison that does not depend on the initial $T_c$, we approximate $\langle L_{\rm core} \rangle \approx (T_c - T_{c,{\rm eq}})(dL/dT_c)_0$, where the derivative is evaluated at the equilibrium point, giving the form $T_c - T_{c,{\rm eq}} = (T_{\rm in} - T_{c,{\rm eq}})e^{-t/\tau}$, where $\tau = 3kM/\mu_i m_p (dL/dT_c)_0$. This $e$-folding time is 0.22, 0.32, 0.45, and 1.9 Gyr for $\langle \dot{M} \rangle = 10^{-8}$, $10^{-9}$, $10^{-10}$, and $10^{-11}\ M_\odot\ {\rm yr}^{-1}$, respectively. If $\langle \dot{M} \rangle$ changes on a timescale shorter than this, $T_c$ will not be maintained at its equilibrium value. In previous work (Bildsten & Townsley 2003), we estimated $(dL/dT_c)_0 \approx 3k\langle \dot{M} \rangle / 2\mu_e m_p$. This estimate matches the results from the full envelope calculations at $\langle \dot{M} \rangle \sim$ a few $\times\ 10^{-11}\ M_\odot\ {\rm yr}^{-1}$, but the actual $\langle \dot{M} \rangle$ dependence is much weaker than estimated because of complications introduced by the varying ignition mechanism and nuclear energy source. For example, heating of the core is relatively less efficient at $\langle \dot{M} \rangle \gtrsim 2 \times 10^{-10}\ M_\odot\ {\rm yr}^{-1}$ when the base of the accreted layer never becomes conductive.

The reheating time at a constant $\langle \dot{M} \rangle$ from a reasonable starting temperature can be calculated directly from equation (10) and the curves in Figure 7 for all but the highest accretion rates. The time for the core of a $0.6\ M_\odot$ C/O WD to heat up from $2.5 \times 10^6$ K, corresponding to a cooling age of 4 Gyr (Salaris et al. 2000), to 90% of the equilibrium temperature is 0.7, 0.9, and 2.4 Gyr for $10^{-9}$, $10^{-10}$, and $10^{-11}\ M_\odot\ {\rm yr}^{-1}$, respectively. The mass that must be transferred in the binary in each of these cases is thus 0.7, 0.09, and 0.024 $M_\odot$. The latter values are quite reasonable expected fluxes in terms of evolution of CVs (see Howell et al. 2001), and thus WDs in CVs with 1.3 hr $< P_{\rm orb} <$ 2 hr are expected to be in equilibrium. However, the flux necessary at $10^{-9}\ M_\odot\ {\rm yr}^{-1}$ is quite high, so that systems with $P_{\rm orb} > 3$ hr are unlikely to have reached equilibrium. This will be mitigated to some degree by the fact that all of the $\sim 0.4\ M_\odot$ transferred above the period gap occurs at $\langle \dot{M} \rangle > 10^{-9}\ M_\odot\ {\rm yr}^{-1}$ (Howell et al. 2001), which has stronger core heating. A system that comes into contact at $P_{\rm orb} \approx 6$ hr should be coming approximately into equilibrium when $P_{\rm orb} \simeq 3$ hr, just above the period gap.

We defer a detailed calculation and discussion relating the evolution of the interacting binary and the thermal state of the WD to a companion paper (Townsley & Bildsten 2003).

## 5. CLASSICAL NOVAE IGNITION MASSES

The principal outcome of our calculations is the equilibrium temperature at which the heating and cooling of the WD core are balanced over the CN cycle. Once this equilibrium has been reached, observable quantities do not depend on the age of the WD but rather on $M$ and $\langle \dot{M} \rangle$, which are determined by the evolution of the binary system.

The top panel of Figure 8 shows $T_{c,\rm eq}$ for a range of $\langle \dot{M} \rangle$ values. Curves for three values of $M$ are shown, two for each with $X_{^3\rm He} = 0.005$ and 0.001, the upper and lower limits on expected values for the accreted material (e.g., D'Antona & Mazzitelli 1982; Iben & Tutukov 1984). The dependence of $T_{c,\rm eq}$ on these parameters is complicated because of the fact that two transitions are taking place over this broad range of accretion rates. There are three regimes. (1) At $\langle \dot{M} \rangle \gtrsim 3 \times 10^{-10}\ M_\odot\ \rm yr^{-1}$, the thermonuclear runaway is well described by a one-zone model, and the dominant nuclear fuel triggering the explosion is $^3$He; $T_{c,\rm eq}$ increases with $\langle \dot{M} \rangle$ in order to balance the higher rate of heat deposition in the envelope. Larger $X_{^3\rm He}$ causes the CN explosion to happen sooner, thus truncating the heating phase relative to lower $X_{^3\rm He}$ and leading to a lower $T_{c,\rm eq}$. The lower limit of this regime depends on $M$ since higher gravity provides a more stable envelope in the one-zone model. (2) At $3 \times 10^{-11} \lesssim \langle \dot{M} \rangle / (M_\odot\ \rm yr^{-1}) \lesssim 3 \times 10^{-10}$, the one-zone model of ignition is no longer sufficient (see § 3), but the dominant nuclear heat source is still $^3$He. The contrast in $T_{c,\rm eq}$ with $M$ has become quite small, while the dependence on $X_{^3\rm He}$ remains. (3) At $\langle \dot{M} \rangle \lesssim 3 \times 10^{-11}\ M_\odot\ \rm yr^{-1}$, the dependence on $X_{^3\rm He}$ is mostly gone and the dominant nuclear heating source is *p-p*.

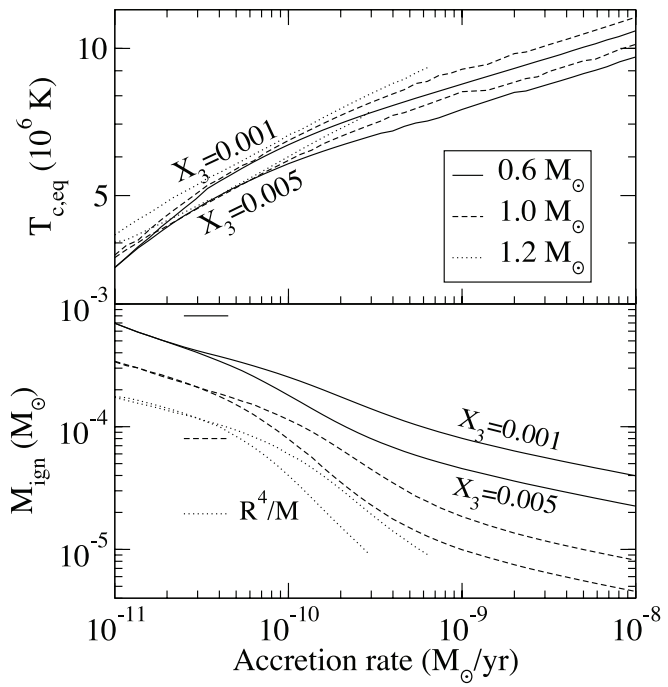


FIG. 8.—Equilibrium core temperature and mass of the accreted layer at CN ignition, $M_{\rm ign}$, as a function of the time-averaged accretion rate $\langle \dot{M} \rangle$. Curves are shown for three WD masses $M$ and two different mass fractions of $^3$He at each value of $M$.

While $T_c$ is not directly observable, the resulting ignition masses $M_{\rm ign}$ can be compared to measured ejection masses. The bottom panel of Figure 8 shows $M_{\rm ign}$ for the equilibrated stars. This is the first self-consistent evaluation of the CN ignition mass, since we use our calculated $T_{c,\rm eq}(\langle \dot{M} \rangle)$. The ignition mass decreases as the mass of the WD increases. This dependence is familiar from previous work but is usually stated as the contrast expected for a constant ignition pressure, $P_{\rm ign} \approx GMM_{\rm ign}/4\pi R^4$, yielding $M_{\rm ign} \propto R^4/M$. Clearly, the ignition pressure for a fixed mass is not constant, since $T_c$ changes with $\langle \dot{M} \rangle$; thus, the simple scaling does not hold.

The contrast in nuclear energy contributions is clearly demonstrated; $^3$He triggering has a pronounced effect on $M_{\rm ign}$ at $\langle \dot{M} \rangle > 10^{-10}\ M_\odot\ \rm yr^{-1}$ and barely any for $\langle \dot{M} \rangle < 4 \times 10^{-11}\ M_\odot\ \rm yr^{-1}$, where *p-p* is the dominant contributor. Our $M_{\rm ign}$ values with $X_{^3\rm He} = 0.001$ are one-half to one-fourth of those found by Fujimoto (1982; see his Fig. 7), the fraction decreasing with increasing $\langle \dot{M} \rangle$. This difference is surprisingly small given that his $\langle \dot{M} \rangle$ values were order-of-magnitude estimates, in contrast to our self-consistent calculations. The grid of CN simulation results in Prialnik & Kovetz (1995) includes values of $M_{\rm ign}$ (their $m_{\rm acc}$) for $M = 0.65$, 1.0, and 1.25 $M_\odot$ and $\langle \dot{M} \rangle = 10^{-10}$, $10^{-9}$, and $10^{-8}\ M_\odot\ \rm yr^{-1}$, with $T_c = 10^7$ K. For $M = 0.6$ and 1.0 $M_\odot$ at $10^{-8}$ and $10^{-9}\ M_\odot\ \rm yr^{-1}$, we find about one-half of their $M_{\rm ign}$ for $X_{^3\rm He} = 0.001$, whereas at $10^{-10}\ M_\odot\ \rm yr^{-1}$, again with $X_{^3\rm He} = 0.001$, we find 1, 1.4, and 3.1 times their $M_{\rm ign}$ at $M = 0.6$, 1.0, and 1.2 $M_\odot$, respectively. We understand these differences as follows. At $\langle \dot{M} \rangle = 10^{-10}\ M_\odot\ \rm yr^{-1}$ our equilibrium temperature is less than $10^7$ K, thus leading to larger ignition masses. Second, our inclusion of $^3$He in the accreted material decreases $M_{\rm ign}$ with respect to calculations that include only CNO enrichment, leading to our lower $M_{\rm ign}$ values at the higher accretion rates where $T_{c,\rm eq}$ is close to $10^7$ K and somewhat counteracting the affect of the lower $T_c$ values at $\langle \dot{M} \rangle = 10^{-10}\ M_\odot\ \rm yr^{-1}$.

Our calculations of $M_{\rm ign}$ agree quite well with those of MacDonald (1984) for $\langle \dot{M} \rangle \lesssim 10^{-10.5}\ M_\odot\ \rm yr^{-1}$. This is where *p-p* burning dominates and the base of the accreted layer is degenerate at ignition. However, his $T_{c,\rm eq}$ values were not reported. At larger $\langle \dot{M} \rangle \sim 10^{-9}$ to $10^{-8}\ M_\odot\ \rm yr^{-1}$, our $M_{\rm ign}$ values are nearly a factor of 10 lower than MacDonald's. This discrepancy is larger than can be explained by $^3$He ignition. As discussed in MacDonald (1983), the "cold" models utilized in MacDonald (1984) leave out one of three ignition conditions. The omitted condition turns out to be quite similar to the one-zone condition and therefore essential at these higher values of $\langle \dot{M} \rangle$.

Accumulated masses are not directly measurable, but the mass ejected in a CN, $M_{\rm ej}$, is known for many systems. A robust comparison between $M_{\rm ign}$ and $M_{\rm ej}$ would tell us whether the WD mass is increasing or decreasing on long timescales during accretion. Because $M_{\rm ign}$ depends on $\langle \dot{M} \rangle$, we must estimate $\langle \dot{M} \rangle$ for a given CN system, requiring us to know the orbital period and to make some presumption about its relationship to $\langle \dot{M} \rangle$. For $P_{\rm orb} < 2$ hr, $\langle \dot{M} \rangle$ is that given by angular momentum loss due to gravitational radiation (Kolb & Baraffe 1999). For $P_{\rm orb} > 3$ hr mass transfer is driven by magnetic braking. To approximate the standard model as presented in, e.g., Howell et al. (2001), we have used two values, $\langle \dot{M} \rangle = 10^{-9}\ M_\odot\ \rm yr^{-1}$ at $P_{\rm orb} = 3$ hr and $\langle \dot{M} \rangle = 10^{-8}\ M_\odot\ \rm yr^{-1}$ at $P_{\rm orb} = 6$ hr. A cross-comparison between $M_{\rm ign}$ and $M_{\rm ej}$ is shown in Figure 9, which shows $M_{\rm ign}$ for $M = 0.6$ and 1.0 $M_\odot$ and $X_{^3\rm He} = 0.001$ and 0.005. The five $M_{\rm ej}$ points, which have large errors, are those systems where both the orbital period and ejected mass

are known. One of these systems, V1974 Cyg, has a kinematic WD mass estimate of 0.75–1.07 $M_\odot$ (Retter, Leibowitz, & Ofek 1997). Other estimates are less certain. Because of the small number of points, large errors, and lack of measured WD masses, the comparison to the current data set is not definitive, but the values do roughly agree, pointing out that most of the accreted mass is ejected during the CN event. We have not found overwhelming evidence for excavation of the WD.

There are now over 50 CNs with measured orbital periods (Warner 2002). Our ignition masses will allow for a calculation of the CN orbital period distribution when combined with CV evolution. For example, the tenfold contrast in ignition mass above and below the period gap makes the CN occurrence rate nearly a factor of 100 lower below the period gap than above. Currently, 10% of the CNs are below the period gap; if these systems all suffer the same selection effects, then the implied population below the period gap is 10 times the number of systems above the period gap.

Our envelope models also predict $T_{\rm eff} = (L/4\pi R^2\sigma_{\rm SB})^{1/4}$, which increases with $M_{\rm acc}$. Figure 10 shows, as a function of $\langle \dot{M} \rangle$ for $T_c = T_{c,\rm eq}$, the range of $T_{\rm eff}$ traversed between $M_{\rm acc} = 0.05M_{\rm ign}$ and $0.95M_{\rm ign}$ for $M = 0.6$, 1.0, and 1.2 $M_\odot$. We find that the surface flux $L$ does not depend strongly on mass, and thus roughly $T_{\rm eff} \propto R^{-1/2}$. Short horizontal lines with this dependence are shown for comparison. The WD $T_{\rm eff}$ has been measured for a number of DN systems when the disk is in quiescence (Sion 1999), and a detailed comparison to such measurements is being published separately (Townsley & Bildsten 2003).

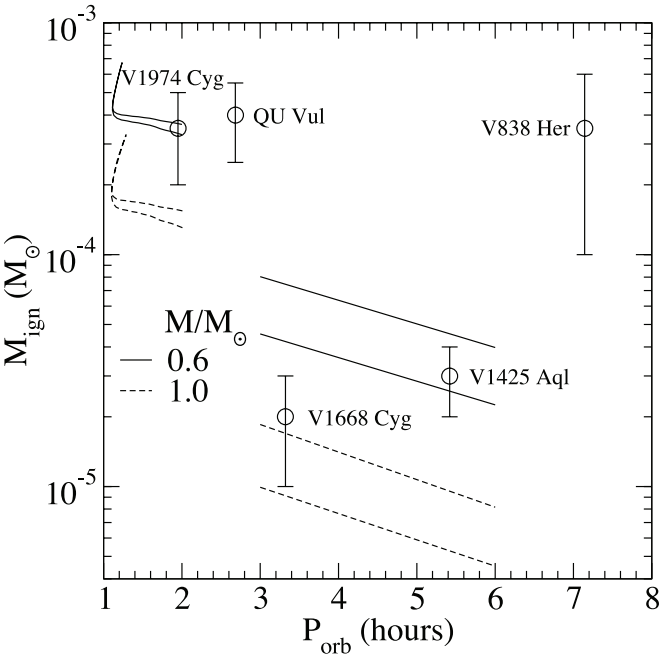


FIG. 9.—Comparison of our predicted CN ignition masses $M_{\rm ign}$ with measurements of CN ejected masses for systems that have a measured orbital period in Warner (2002). The ejected mass references are as follows: V1974 Cyg, Gehrz et al. (1998); QU Vul, Shin et al. (1998); V1668 Cyg, Gehrz et al. (1998); V1425 Aql, Lyke et al. (2001); and V838 Her, Gehrz et al. (1998). The two lines at each value of $M$ as indicated are for $X_{^3\rm He} = 0.001$ and 0.005, giving larger and smaller values, respectively, of $M_{\rm ign}$. At low periods, $\langle \dot{M} \rangle$ is that expected from gravitational radiation (Kolb & Baraffe 1999), and at $P_{\rm orb} = 3$ and 6 hr, we use $\langle \dot{M} \rangle = 10^{-9}$ and $10^{-8}$ $M_\odot$ yr$^{-1}$, respectively, which is approximately the value expected above the period gap due to magnetic braking (Howell et al. 2001).

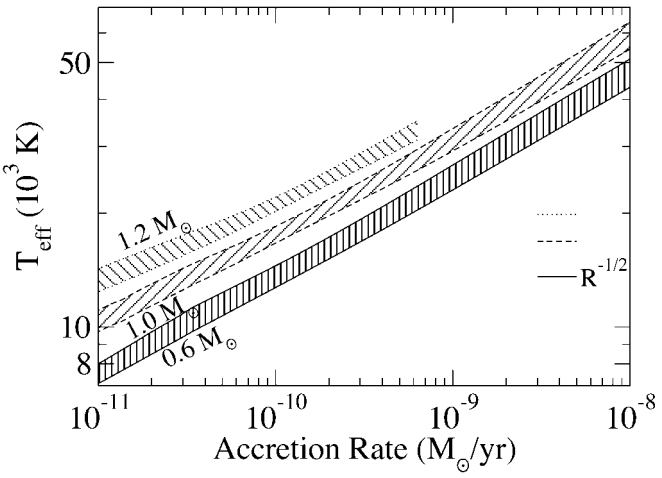


FIG. 10.—Ranges of WD $T_{\rm eff}$ as a function of accretion rate for WD mass $M = 0.6$, 1.0, and 1.2 $M_\odot$ (*bottom to top*). The minimum is evaluated when $M_{\rm acc} = 0.05M_{\rm ign}$ and the maximum when $M_{\rm acc} = 0.95M_{\rm ign}$. For comparison, in 1 Gyr a 0.6 or 1.0 $M_\odot$ isolated WD cools to $T_{\rm eff} = 9 \times 10^3$ or $14 \times 10^3$ K, respectively (Salaris et al. 2000).

## 6. CONCLUSION AND DISCUSSION

A quasi-static WD envelope model has been used to find the equilibrium core temperature $T_{c,\rm eq}$ of an accreting WD under the approximation that exactly the accreted layer is ejected in each CN outburst. Such an equilibrium can be reached in $\lesssim$1 Gyr, allowing for CVs to come close to equilibrium by the time they reach $P_{\rm orb} \simeq 3$ hr and insuring equilibration for $P_{\rm orb} < 2$ hr. Having solved for $T_{c,\rm eq}$, it is then possible to predict the CN ignition mass $M_{\rm ign}$ and the thermal contribution to the WD $T_{\rm eff}$. This is the first determination of $M_{\rm ign}$ that utilizes a WD state determined from $\langle \dot{M} \rangle$ and the cooling and heating of the core during the CN buildup, making it fully self-consistent. When comparing with several papers from the CN literature (Fujimoto 1982; Prialnik & Kovetz 1995; MacDonald 1984), we find that the inclusion of $^3$He leads to lower values of $M_{\rm ign}$ for $\langle \dot{M} \rangle \gtrsim 10^{-10}$ $M_\odot$ yr$^{-1}$ and that for values of $\langle \dot{M} \rangle$ below this, the particular author's assumption concerning $T_c$, which we calculate consistently, is a determining factor. When compared with observed ejected masses, our $M_{\rm ign}$ values are compatible with $M_{\rm ej} \simeq M_{\rm ign}$. Had this comparison favored either $M_{\rm ej} > M_{\rm ign}$ or the opposite, the equilibrium would take place at some $T_c$ such that $L_{\rm core}$ has the value appropriate for the implied secular change in core mass, which can be calculated using the formalism presented in Appendix A.

Over 20 DNs have been observed in quiescence, when the accretion rate is low, the WD photosphere is detected, and $T_{\rm eff}$ is measured. The theoretical work presented here is compared to these observations in Townsley & Bildsten (2003), allowing us to constrain the WD mass and the time-averaged accretion rate $\langle \dot{M} \rangle$. We show there, for systems with $P_{\rm orb} \lesssim 2$ hr, that if $\langle \dot{M} \rangle$ is given by gravitational radiation losses alone, then the WD masses are greater than 0.8 $M_\odot$. An alternative conclusion is that the masses are closer to 0.6 $M_\odot$ and $\langle \dot{M} \rangle$ is 3–4 times larger than that expected from gravitational radiation losses.

It is well known that an isolated WD will pulsate when its $T_{\rm eff}$ value is in the approximate range 11,000–12,000 K (Bergeron

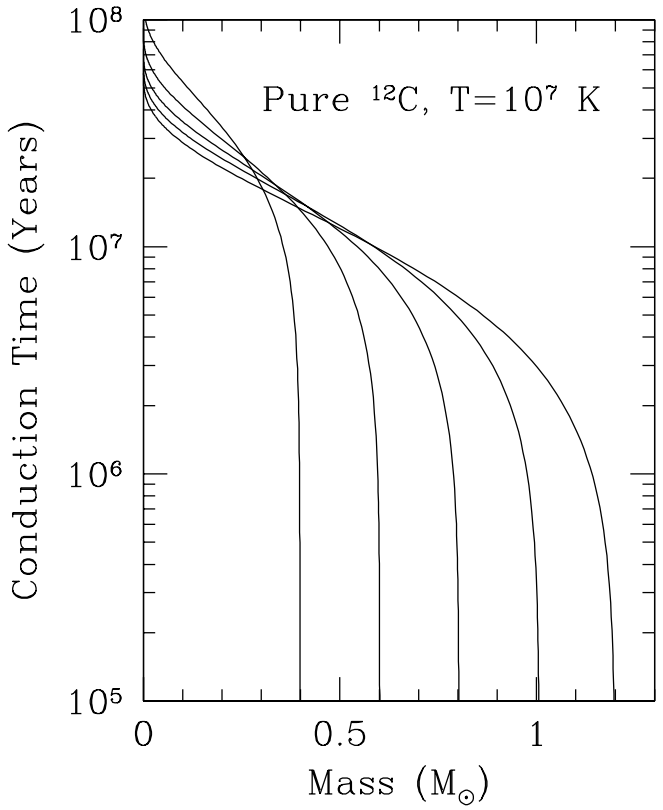


FIG. 11.—Thermal conduction time ($t_{\rm cond}$ in eq. [A2]) from the exterior of a pure carbon WD to an interior mass point. The curves are for isothermal WDs ($T = 10^7$ K) with masses $M = 0.4$, 0.6, 0.8, 1.0, and 1.2 $M_\odot$.

et al. 1995). While a difference in the atmospheric composition—H/He mixture under accretion versus pure hydrogen in the nonaccreting case—will shift this range, it is likely that a similar pulsation mechanism will be active in accreting WDs. Our calculations indicate that accreting WDs with $M = 0.6$–$1.0\ M_\odot$ should be near this range when $\langle \dot{M} \rangle =$ a few $\times\ 10^{-11}\ M_\odot\ {\rm yr}^{-1}$ (see Fig. 10). This value of $\langle \dot{M} \rangle$ is typical of those expected in CVs when accretion is driven by emission of gravitational radiation, $P_{\rm orb} < 2$ hr (Kolb & Baraffe 1999). In fact, one system, GW Lib, has been found that does exhibit precisely this type of variability (van Zyl et al. 2000; Szkody et al. 2002). Using the interior models developed here, we are now undertaking a seismological study of these systems. This offers the tantalizing possibility of facilitating measurement of the WD mass and spin and determination of gross internal structural features such as the size of the accreted layer.

We thank Ed Sion for numerous conversations, Paula Szkody for up-to-date information on the DN observations, Brad Hansen for insights on modern WD modeling, Francesca D'Antona for questioning our equilibria, and the referee for constructive criticism. This research was supported by the National Science Foundation under grants PHY 99-07949 and AST 02-05956. Support for this work was provided by NASA through grant AR-09517.01-A from STScI, which is operated by AURA, Inc., under NASA contract NAS5-26555. D. T. is an NSF Graduate Fellow, and L. B. is a Cottrell Scholar of the Research Corporation.

## APPENDIX A

## THE THERMAL STATE OF THE UNDERLYING WHITE DWARF

The thermal state of the WD core can affect the envelope structure through the heat flow into or out of it on the evolutionary times we are considering. Because of varying ejected mass in CN outbursts, we do not actually know whether the WD core is increasing or decreasing in mass. However, we show here that for a C/O core, the compression or decompression rate of the WD core will have little impact on the overall envelope calculations. This is less clear for those WDs with pure helium cores that are likely present in binaries below the period gap (e.g., Howell et al. 2001). Our discussion follows closely the insights of Nomoto & Sugimoto (1977), Nomoto (1982), and Hernanz et al. (1988).

The WDs of interest here consist mostly of $^{12}$C and $^{16}$O, so we construct the deep interior (far beneath the freshly accreted hydrogen and helium) using the degenerate electron equation of state for $\mu_e = 2$, neglecting the small $^{22}$Ne fraction. The ions completely dominate the thermodynamics and thermal conductivity of the liquid WD interior. For a classical one-component plasma with ion separation $a$ defined by $a^3 = 3/4\pi n_i$, where $n_i = \rho/Am_p$, the importance of Coulomb physics for the ions is measured by

$$\Gamma \equiv \frac{(Ze)^2}{akT} = 57.7\rho_6^{1/3}\left(\frac{10^7\ {\rm K}}{T}\right)\left(\frac{Z}{8}\right)^2\left(\frac{16}{A}\right)^{1/3}, \tag{A1}$$

where $\rho_6 = \rho/10^6$ g cm$^{-3}$. We work in the liquid regime, $\Gamma < 175$ (Potekhin & Chabrier 2000 and references therein). For a 0.6 or 1.2 $M_\odot$ pure oxygen WD, this requires that the core temperature $T_c$ exceed 5 or $16 \times 10^6$ K, respectively (this is within the range expected for the low-mass WDs from § 5). Following the recent work of DeWitt, Slattery, & Chabrier (1996) and Chabrier & Potekhin (1998), we use the linear sum rule to evaluate the Coulomb energy in the mixed liquid phase and the resulting specific heat $c_V$. We then integrate throughout the stellar model to find the total heat capacity of the white dwarf, $C_V = \int c_V\, dM$, as a function of the isothermal WD temperature. In agreement with Potekhin & Chabrier (2000), we find that $C_V$ is nearly that of a classical crystal, $C_V = 3k(M/\mu_i m_p)$, for temperatures in the range of the melting value and slightly above and below.

Electron conduction dominates the heat transport in the deep liquid WD interior, and we use the work of Yakovlev & Urpin (1980) for our estimates of the thermal conductivity $K$ when electron-ion collisions dominate. For an isothermal WD, the time it takes for conduction to transport heat from the outside edge $R$ to an interior radius $r$ is

$$t_{\rm cond} = \frac{1}{4}\left[\int_r^R \left(\frac{c_V}{\rho K}\right)^{1/2} \rho\, dr\right]^2 , \tag{A2}$$

as shown by Henyey & L'Ecuyer (1969). This is simply a slightly more sophisticated version of what Nomoto & Sugimoto (1977) call $\tau_h = c_V \rho H_p^2/K$, the time for heat transport across a pressure scale height $H_p$. Since $c_V$ is nearly independent of temperature, the main $T$ scaling of $t_{\rm cond}$ is from the conductivity, yielding $t_{\rm cond} \propto 1/T$. Figure 11 plots $t_{\rm cond}$ as a function of the mass location within pure, isothermal ($T = 10^7$ K) carbon WDs of masses $M = 0.4,\ 0.6,\ 0.8,\ 1.0$, and $1.2\ M_\odot$. The timescale is only slightly different for pure oxygen WDs.

The compression of the WD interior is adiabatic if accretion compresses it on a timescale much shorter than $t_{\rm cond} \approx (2\text{–}4)\times 10^7(10^7\ {\rm K}/T)$ yr. To relate the compression rate to $\dot{M}$, we start at the WD core and write $d\ln\rho_c/dt = (d\ln\rho_c/d\ln M)d\ln M/dt$ (e.g., Nomoto 1982). For a low-mass WD, $\alpha = d\ln\rho_c/d\ln M = 2$, but $\alpha$ increases as $M$ approaches the Chandrasekhar mass, having values of $\alpha = 3.27,\ 4.26,\ 6.17$, and 10.71 for $M = 0.6,\ 0.8,\ 1.0$, and $1.2\ M_\odot$. For example, the accretion rate required to adiabatically compress the interior of a $0.8\ M_\odot$ WD when $T = 10^7$ K is greater than $6\times 10^{-9}\ M_\odot\ {\rm yr}^{-1}$. Simulations for rates this rapid have been carried out (e.g., Nomoto & Iben 1985) and clearly show the central adiabatic compression. Since the ions dominate the entropy there, we calculate the adiabat in the liquid state using the internal energy given by Chabrier & Potekhin (1998) to find

$$\left(\frac{d\ln T}{d\ln\rho}\right)_{\rm ad} \approx \frac{0.91 + 0.14\Gamma^{1/3}}{1.22 + 0.41\Gamma^{1/3}} , \tag{A3}$$

within 1% of the adiabat given by Hernanz et al. (1988) for $\Gamma > 1$ to crystallization. For accretion rates where the compression time and conduction time are comparable, there is clearly time for heat to be transported but not adequate time for maintaining an isothermal core.

However, for $\dot{M} \ll 6\times 10^{-9}\ M_\odot\ {\rm yr}^{-1}$, there is time for the core to remain isothermal under the compression (Hernanz et al. 1988), simplifying the treatment of the WD core for the values of $\dot{M}$ of most interest to us. Unlike our treatment of the atmosphere, for the deep interior we need to account for the changing global structure of the WD. Nomoto (1982) showed that this is greatly simplified by rewriting the entropy equation in terms of the variable $q = M_r/M$, where $M_r$ is the mass interior to $r$ and $M$ is the total mass. Under accretion, we relate $\dot{q}/q = \dot{M}_r/M_r - \dot{M}/M$ and rewrite the time derivative as $d/dt = \partial/\partial t|_q + \dot{q}\partial/\partial q|_t$. In the entropy equation, we want the Lagrangian time derivative $d/dt|_{M_r}$, so that $\dot{q} = -q\dot{M}/M$ and the entropy equation simply becomes

$$T\left(\frac{\partial s}{\partial t}\right)_q - T\frac{d\ln M}{dt}\left(\frac{\partial s}{\partial \ln q}\right)_t = -\frac{\partial L_r}{\partial M_r} \tag{A4}$$

under the action of compression. Integrating this equation tells us the luminosity exiting the surface of the WD core

$$L = \frac{d\ln M}{d\ln t}\int_0^M T\left(\frac{\partial s}{\partial \ln q}\right)_t dM_r - \int_0^M T\left(\frac{\partial s}{\partial t}\right)_q dM_r , \tag{A5}$$

as clearly written by Nomoto & Sugimoto (1977).

The advantage to writing the terms in this manner becomes apparent once we use

$$ds = \frac{k}{\mu_i m_p}\left(a\, d\ln T - b\, d\ln\rho\right) , \tag{A6}$$

where $a = 1.22 + 0.41\Gamma^{1/3}$ and $b = 0.91 + 0.14\Gamma^{1/3}$ are presumed to be roughly constant throughout the WD. If the ions were an ideal gas, we would have $a = 3/2$ and $b = 1$. Presuming that the WD core is always isothermal at $T = T_c$, equation (A5) then becomes

$$L\frac{\mu_i m_p}{kT_c} = -\frac{d\ln M}{dt}\int_0^M b\left(\frac{d\ln\rho}{d\ln q}\right)_t dM_r - aM\frac{d\ln T_c}{dt} + \int_0^M b\left(\frac{d\ln\rho}{d\ln M}\right)_q \frac{d\ln M}{dt}\, dM_r . \tag{A7}$$

We can rewrite this more clearly by regrouping terms to obtain

$$L + \frac{aMk}{\mu_i m_p}\frac{dT_c}{dt} = -\frac{bkT_c}{\mu_i m_p}\frac{d\ln M}{dt}\int_0^M \left[\left(\frac{d\ln\rho}{d\ln q}\right)_t - \left(\frac{d\ln\rho}{d\ln M}\right)_q\right] dM_r . \tag{A8}$$

The term $d\ln\rho/d\ln M|_q$ is the generalization of the piece discussed earlier in the context of the central point. It gives the compression rate at a fixed mass coordinate $q$ due to accretion. Nomoto (1982) showed that it is independent of $q$ within the deep interior, so that $\alpha = d\ln\rho_c/d\ln M \approx d\ln\rho/d\ln M|_q$ and equation (A8) becomes

$$L + \frac{aMk}{\mu_i m_p}\frac{dT_c}{dt} = \frac{\alpha bkT_c}{\mu_i m_p}\frac{dM}{dt} - \frac{bkT_c}{\mu_i m_p}\frac{d\ln M}{dt}\int_0^M M_r d\ln\rho\,, \tag{A9}$$

where the last term becomes large near the surface and is evaluated in Appendix B as part of the outer envelope integration (see eq. [B3]). At $\Gamma \approx 80$, $a = 3$ and $b = 1.5$, so for a $M = 0.8\ M_\odot$ WD we get the simple relation for compression of the deep interior of the WD

$$L + \frac{aMk}{\mu_i m_p}\frac{dT_c}{dt} = \frac{6.4kT_c}{\mu_i m_p}\frac{dM}{dt}\,, \tag{A10}$$

implying that the core can remain at a fixed temperature during compression from accretion as long as the exiting luminosity is

$$L_{\rm core} = \frac{6.4kT_c}{\mu_i m_p}\frac{dM}{dt}\,. \tag{A11}$$

Comparison of this with the corresponding estimate for the accreted layers from Appendix B, equation (B4), demonstrates that even if the WD core is accumulating mass on a secular timescale (i.e., no ejection of matter), then, since $\mu_i \approx 14$, such an exiting luminosity as $L_{\rm core}$ would be a small perturbation on the thermal state of the envelope. This statement would change for a helium WD, where $\mu_i = 4$, in which case the core luminosity could modify the envelope structure.

## APPENDIX B

## ANALYTICAL ENVELOPE INTEGRATION

Here we present the integration of equation (3) from § 2 using a simple model for a WD consisting of a radiative outer envelope and a degenerate deeper layer that is isothermal. Dropping the nuclear burning and the time derivative term from equation (1) leads to the integral

$$L = \langle\dot{M}\rangle\int_0^P T\frac{ds}{dP}\,dP\,. \tag{B1}$$

To allow a simple integration, in the envelope we make the approximation that the luminosity is constant with depth and that the opacity has the form $\kappa \propto \rho T^{-3.5}$ so that $P^2 \propto T^{8.5}$. The entropy of an ideal gas is $s = k\ln(T^{3/2}/\rho)/\mu m_p$, which can be expressed in terms of pressure alone, allowing evaluation of $ds/dP$, and

$$L_{\rm env} = 0.41\frac{k}{\mu m_p}\langle\dot{M}\rangle\int T\frac{dP}{P} = 1.75\langle\dot{M}\rangle\frac{kT_c}{\mu m_p}\,, \tag{B2}$$

where $P^2 \propto T^{8.5}$ has been used to evaluate the integral, the term from the outer boundary has been dropped, and the pressure at the inner boundary (the transition to degeneracy) has been written in terms of $T_c$.

The degenerate section is nearly isothermal and the entropy is completely in the ions, so that $s = k\ln(T^{3/2}/\rho)/\mu_i m_p$, and the density is related to the pressure by $P \propto \rho^{5/3}$ from the surrounding nonrelativistic degenerate electrons. From this $ds/dP$ can be evaluated, but some limits must be chosen. The lower limit is the pressure at which the transition to degeneracy occurs; this is simply $P_{\rm tr} = T_c^{5/2}$ in cgs units for a solar mixture. The upper limit is the pressure at the base of the accreted envelope $P_{\rm base} = gM_{\rm acc}/4\pi R^2$. From our results, at $\langle\dot{M}\rangle = 10^{-10}\ M_\odot\ {\rm yr}^{-1}$, $T_c = 8\times10^6$ K and $M_{\rm ign} = 3\times10^{-4}\ M_\odot$. Using these values gives $P_{\rm tr} = 1.8\times10^{17}$ ergs cm$^{-3}$ and $P_{\rm base} = 6.5\times10^{18}$ ergs cm$^{-3}$ and thus

$$L_{\rm deg} = \frac{3}{5}\frac{kT_c}{\mu_i m_p}\langle\dot{M}\rangle\int d\ln P = 2.15\langle\dot{M}\rangle\frac{kT_c}{\mu_i m_p}\,. \tag{B3}$$

Although the limits taken actually depend on $T_c$, they appear in a logarithm, so only the strongest temperature dependence is shown explicitly. Using $\mu/\mu_i = 0.6/1.3$ for solar material to eliminate $\mu_i$ and adding the luminosity from the nondegenerate and degenerate portions of the accreted layer gives

$$L \approx \frac{3\langle\dot{M}\rangle kT_c}{\mu m_p}\,. \tag{B4}$$

This fiducial estimate of the compressional heating proves helpful in our analytic understanding of our initial results.

REFERENCES

Alcock, C., & Illarionov, A. 1980, ApJ, 235, 534
Althaus, L. G., & Benvenuto, O. G. 1997, ApJ, 477, 313
Bergeron, P., Wesemael, F., Lamontagne, R., Fontaine, G., Saffer, R. A., & Allard, N. F. 1995, ApJ, 449, 258
Bildsten, L., & Townsley, D. M. 2003, in White Dwarfs, ed. D. De Martino et al. (NATO Sci. Ser. II, 105; Dordrecht: Kluwer), 313
Caughlan, G. R., & Fowler, W. A. 1988, At. Data Nucl. Data Tables, 40, 283
Chabrier, G., Brassard, P., Fontaine, G., & Saumon, D. 2000, ApJ, 543, 216
Chabrier, G., & Potekhin, A. Y. 1998, Phys. Rev. E, 58, 4941
Clayton, D. D. 1983, Principles of Stellar Evolution and Nucleosynthesis (Chicago: Univ. Chicago Press)
D'Antona, F., & Mazzitelli, I. 1982, ApJ, 260, 722
Deloye, C., & Bildsten, L. 2002, ApJ, 580, 1077
DeWitt, H., Slattery, W., & Chabrier, G. 1996, Physica B, 228, 21
Diaz, M. P., & Bruch, A. 1997, A&A, 322, 807
Farouki, R. T., & Hamaguchi, S. 1993, Phys. Rev. E, 47, 4330
Fontaine, G., Brassard, P., & Bergeron, P. 2001, PASP, 113, 409
Fujimoto, F. Y. 1982, ApJ, 257, 767
Fujimoto, M. Y., Hanawa, T., & Miyaji, S. 1981, ApJ, 247, 267
Gehrz, R. D., Truran, J. W., Williams, R. E., & Starrfield, S. 1998, PASP, 110, 3
Godon, P., & Sion, E. M. 2002, ApJ, 566, 1084
Hansen, B. M. S. 1999, ApJ, 520, 680
Henyey, L., & L'Ecuyer, J. 1969, ApJ, 156, 549
Hernanz, M., Isern, J., Canal, R., Labay, J., & Mochkovitch, R. 1988, ApJ, 324, 331
Howell, S. B., Nelson, L. A., & Rappaport, S. 2001, ApJ, 550, 897
Iben, I., Jr., Fujimoto, M. Y., & MacDonald, J. 1992a, ApJ, 384, 580
———. 1992b, ApJ, 388, 521
Iben, I., Jr., & MacDonald, J. 1985, ApJ, 296, 540
Iben, I., Jr., & Tutukov, A. V. 1984, ApJ, 284, 719
Ichimaru, S. 1993, Rev. Mod. Phys., 65, 255
Iglesias, C. A., & Rogers, F. J. 1996, ApJ, 464, 943
Itoh, N., Mitake, S., Iyetomi, H., & Ichimaru, S. 1983, ApJ, 273, 774
Kolb, U., & Baraffe, I. 1999, MNRAS, 309, 1034
Lyke, J. E., et al. 2001, AJ, 122, 3305
MacDonald, J. 1983, ApJ, 267, 732
———. 1984, ApJ, 283, 241
Mestel, L. 1952, MNRAS, 112, 583
Nomoto, K. 1982, ApJ, 253, 798
Nomoto, K., & Iben, I. 1985, ApJ, 297, 531
Nomoto, K., & Sugimoto, D. 1977, PASJ, 29, 765
Ogata, S., Iyetomi, H., & Ichimaru, S. 1991, ApJ, 372, 259
Paczyński, B. 1983, ApJ, 267, 315
Paquette, C., Pelletier, C., Fontaine, G., & Michaud, G. 1986, ApJS, 61, 177
Potekhin, A. Y., & Chabrier, G. 2000, Phys. Rev. E, 62, 8554
Prialnik, D., & Kovetz, A. 1995, ApJ, 445, 789
Pringle, J. E. 1988, MNRAS, 230, 587
Retter, A., Leibowitz, E. M., & Ofek, E. O. 1997, MNRAS, 286, 745
Salaris, M., García-Berro, E., Hernanz, M., Isern, J., & Saumon, D. 2000, ApJ, 544, 1036
Shin, J.-Y., Gehrz, R. D., Jones, T. J., Krautter, J., Heidt, J., & Hjellming, R. M. 1998, AJ, 116, 1966
Sion, E. M. 1995, ApJ, 438, 876
———. 1999, PASP, 111, 532
Szkody, P., Gäsicke, B. T., Howell, S. B., & Sion, E. M. 2002, ApJ, 575, L79
Townsley, D. M., & Bildsten, L. 2002, ApJ, 565, L35
———. 2003, ApJ, 596, L227
van Zyl, L., Warner, B., O'Donoghue, D., Sullivan, D., Pritchard, J., & Kemp, J. 2000, Baltic Astron., 9, 231
Wallenborn, J., & Baus, M. 1978, Phys. Rev. A, 18, 1737
Warner, B. 1995, Cataclysmic Variable Stars (Cambridge: Cambridge Univ. Press)
———. 2002, in AIP Conf. Proc. 637, Classical Nova Explosions, ed. M. Hernanz & J. José (Melville: AIP), 3
Wood, M. A. 1995, in White Dwarfs, ed. D. Koester & K. Werner (Berlin: Springer), 41
Yakovlev, D. G., & Urpin, V. A. 1980, Soviet Astron., 24, 303